Int J Adv Manuf Technol (2017) 88:229–240
DOI 10.1007/s00170-016-8779-x

ORIGINAL ARTICLE

The effect of combining high-intensity ultrasonic vibration with ECAE process on the process parameters and mechanical properties and microstructure of aluminum 1050

Saeed Bagherzadeh[1,2] · **Karen Abrinia**[1] · **Yanfei Liu**[2] · **Qingyou Han**[2]

Received: 9 January 2016 / Accepted: 12 April 2016 / Published online: 22 April 2016

Abstract Equal channel angular extrusion, as one most common severe plastic deformation method for producing ultra-fine grain materials, has some limitations such as high forming load, high friction forces, microstructure inhomogeneity, and a large number of passes required for obtaining fine-grained structure. The main goal of this research is investigation on the effect of using high-intensity ultrasonic vibration directly in the plastic deformation zone during the ECAE process of commercially pure aluminum 1050 to improve process limitations. By combining ultrasonic vibration with the ECAE, the sample with nearly equiaxed grains and average size ~2 μm was achieved just after one pass more effective than two passes of conventional ECAE via routes C and Bc. Accordingly, the samples with 22 % higher hardness, 10 % more compressive strength, and also 30 % lower required forming load were attained during ultrasonic-assisted ECAE with applied vibration amplitude 15 μm.

Keywords Equal channel angular extrusion · Ultrasonic · Microstructure · Mechanical properties · Forming force

✉ Saeed Bagherzadeh
S_bagherzadeh@ut.ac.ir

[1] School of Mechanical Engineering, College of Engineering, University of Tehran, North Kargar Ave., North Amirabad, PO. Box: 11155-4563, Tehran, Iran

[2] Department of Mechanical Engineering Technology, Purdue University, 401 North Grant Street, West Lafayette, IN 47906, USA

1 Introduction

The interest to research about production of ultra-fined grain (UFG) and nano-structured (NS) materials has been increasingly developed during the last decade. It is well-known that mechanical properties of materials can be improved by grain refining based on Hall-Petch equation [1]. This goal can be obtained by severe plastic deformation (SPD) processes by imposing high shear strain during plastic deformation of metals. One of the most common SPD methods is equal channel angular extrusion (ECAE), which was first introduced by Segal [2]. However, it has some limitations such as high forming force, limitation in sample size, several passes required to reach a reasonable UFG structure, high friction forces, inhomogeneity of microstructure and strain distribution, etc. [3]. Therefore, it is of interest to promote efficiency of conventional ECAE process.

On the other hand, the application of ultrasonic vibration (UV) as a high-frequency mechanical wave in manufacturing processes has taken into consideration because of remarkable effects on process and material properties [4]. The influence of superimposed UV on plastic deformation of metals has been studied from two aspects of surface effect and volume effect [5]. The surface effect is revealed by reduction of friction forces between vibrated tool and specimen and one more important volume effect, which relates to change in internal parameters such as mechanical properties and microstructural characteristics of metals. Formerly, these effects have been observed during ultrasonic-assisted compression and tension tests obviously [6]. Based on that, the superimposed UV can remarkably soften the metal during plastic deformation as a temporary effect (Blaha effect), which is entitled acoustic softening and also flow stress recovery that occurs after UV stoppage so-called acoustic residual hardening [7]. These acoustic effects can be beneficial to improve limitations of metal-

forming processes. There have been only a limited number of reports to date about ultrasonic-assisted metal forming processes [8]. Jimma et al. [9] found that limiting drawing ratio (LDR) increased and forming load and friction force decreased by using ultrasonic vibration during deep drawing. Bunget and Ngaile [10] showed potential effect of ultrasonic vibration in reducing forming load and surface finish enhancement in the micro-extrusion. Although the main goal of the most previously presented reports has been the reduction of forming force and improvement of formability by ultrasonic surface effect, a few efforts have been established to improve mechanical properties and microstructure of materials by using UV. Han et al. [11] established a novel method for producing nanostructured metal by using ultrasonic-assisted upsetting (UAU). They attained copper with grain size about 100 nm in the severe deformed tip. Wen et al. [12] conducted tensile tests on AZ31 using ultrasonic vibration. They observed a notable change in the microstructure of fractured and deformed section regions on samples after ultrasonically assisted tensile tests. In addition, they claimed that the softening phenomenon occurs during plastic deformation in low ultrasonic energy against fragile behavior of material when high energy of UV is applied. Siu et al. [13] carried out experimental studies on ultrasonic-assisted micro-indentation (UAI) on aluminum samples. They reported an increase in diagonal length of indented zone and typical softening of specimen during process. In addition, they observed subgrain formation with size about 1–2 μm by transmission electron microscopy (TEM) on the surface of UAIed samples. Liu et al. [14] established a novel combined method upsetting with ultrasonic vibration (UUV) to get nano-scaled material grains. They observed high plastic strain occurred on cone-shaped copper sample when ultrasonic wave was imposed on sample directly. Moreover, TEM images revealed subgrain formation with grain size in range of 100–300 nm efficiently similar to SPD methods. Han [15] has published a review paper to conclude their findings on the effect of using UV for degassing of molten aluminum, particulate-reinforced metal matrix composites processing, refining metals and alloys during solidification process and welding, and producing bulk nanostructures in solid metals and alloys. The results show capability of UV to degassing, grain refining, and inducing NS materials in solid metals clearly. Djavanroodi et al. [16] made an attempt to numerical modeling and experiment of ultrasonic-assisted ECAP process by using a vibrated forming punch on billet. They reported just a maximum 9 % reduction in forming force due to surface effect without any investigation on neither the mechanical properties nor the microstructural changes. Their design was not robust adequately because of ultrasonic wave dissipation was occurred through billet length without achieving to resonance condition in the main deformation zone.

In the new proposed method, the high-intensity ultrasonic vibration with frequency f and vibration amplitude λ is imposed in the plastic deformation zone (PDZ) of ECAE process, the so-called ultrasonic-assisted ECAE (UE). Unlike the conventional ECAE process, the new developed die had three channels including billet input channel, product output channel, and a new cylindrical channel for ultrasound horn inlet. In this process, the punch pushes the billet through the die channel while it experiences a high-intensity ultrasonic vibration in the PDZ by mean of vibrated horn. The billet in the PDZ can be excited by ultrasonic wave in two separate directions as laterally or vertically than extrusion direction (ED), as shown schematically in Fig. 1a, b, which are called L-UE and V-UE methods respectively. Investigation on deformation behavior of metal in the PDZ during UE process can help to find out the role of superimposed ultrasonic vibration.

A comparative analysis between ECAE method without and with ultrasonic energy can be drawn by investigation on deformation behavior of metal in plastic deformation zone. The material elements in the PDZ experiences compression and shear in both x- and y-axis and also a large rigid body rotation, maximum at the symmetry plane of the flow at 45°; however, the shear mode is the main deformation mechanism. The equivalent strain rate ($\dot{\varepsilon}_{eq}$) elements in the PDZ can be calculated from components of strain rate by:

$$\dot{\varepsilon}_{eq} = \sqrt{\left(2/3\right)\dot{\varepsilon}_{ij}\dot{\varepsilon}_{ij}} \tag{1}$$

Where ε_{ij} is the strain rate increment component. Now, in the proposed method, the material particles in PDZ also experience a superimposed ultrasonic vibration as a high impact pressure which can cause variation in strain rate of components [17]. As mentioned in literatures, this change as volume effect can explain in microscopic scale. The variation of plastic strain rate as shear type ($\dot{\gamma}$) can be described by crystal plasticity theory with considering acoustic softening phenomenon. The modified evolution law in a special slip system (α) was introduced by [18]:

$$\dot{\gamma}^{(\alpha)} = \dot{\gamma}_0{}^{(\alpha)}.sgn\left(\tau^{(\alpha)}\right)\left\{\left|\frac{\tau^{(\alpha)}}{g^{(\alpha)}.U_{soft}}\right|\right\}^m \tag{2}$$

Where $\tau^{(\alpha)}$ is resolved shear stress and $\dot{\gamma}_0{}^{(\alpha)}$ and m are reference strain rate and sensitivity exponent related to material properties and $g^{(\alpha)}$ is strength of slip system (α). U_{soft} is ultrasonic softening coefficient with value smaller than 1 that shows ultrasonic energy effect on soften down of material during deformation. Hence, combining ultrasonic vibration during plastic deformation of material elements in the PDZ can promote amount of strain and strain rates. From macroscopic viewpoint, the acoustic softening of material in the plastic deformation zone under ultrasonic excitation causes a decrease in flow stress of material in the PDZ as reported by literatures [4, 6, 7, 19]. In addition, applying ultrasonic

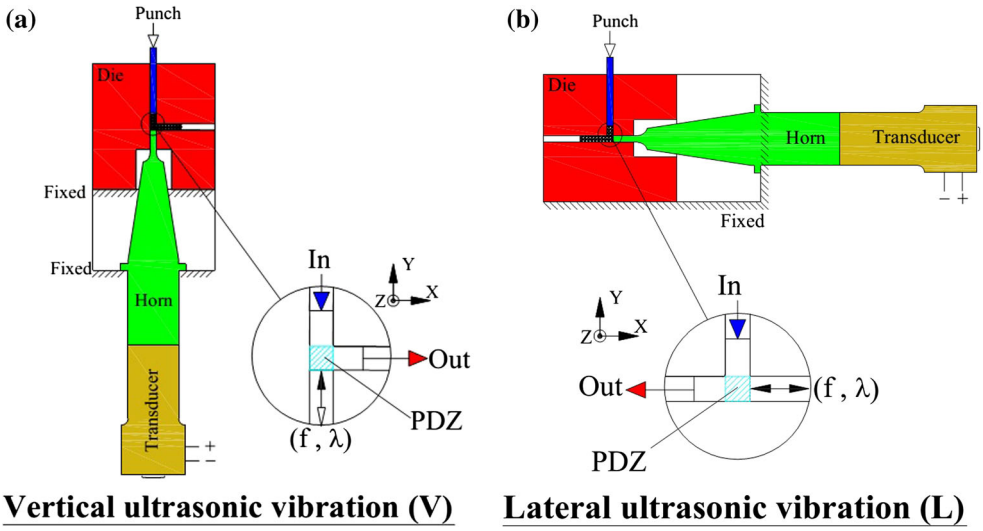

Fig. 1 The schematic diagrams of combining ultrasonic vibration with ECAE process: **a** vertical vibration parallel to extrusion direction and **b** lateral vibration perpendicular to extrusion direction

vibration on billet can cause a decrease in friction forces between material and die wall and vibrated surface (as seen in Fig. 1) that has been studied for sliding friction by Hess and Soom [20] and Kumar and Hutchings [21] for normal and in-plane ultrasonic vibration in details.

To improve efficiency of ECAE method, the authors have established UE technique to apply high-intensity ultrasonic vibration on the ECAE. For this purpose, the authors have confined the research to comparative study on required forming force, mechanical strength, hardness, and microstructural evolution of pure aluminum deformed by new proposed method. Accordingly, the experimental setup was designed to examine pure aluminum samples. Discussion on the obtained results can reveal the role of applying high-intensity UV on ECAE process clearly.

2 Experiments

2.1 Material

The experimental samples from commercially pure aluminum (AA 1050) were cut and machined from sheet as 5×5 mm^2 section bars with 30 mm length. Then, the test specimens were prepared by full annealing process at 623°K for 2 h with furnace cooling to reach nearly equiaxed coarse grains. Table 1 indicates the chemical composition and mechanical properties of as-annealed aluminum sample. Of course, the mechanical properties of aluminum changes during ultrasonic irradiation as softening behavior and also after ultrasonic stoppage as residual hardening. The compression behavior of proposed aluminum samples under ultrasonic excitation in different vibration amplitudes has been studied in Ref [6] in details.

2.2 Tooling design

According to sample size, the punch made of steel SPK and the die channels were machined from hot-worked steel AISI H13 by using electrical discharge machining and milling and then surface hardened. The die (φ) and corner angles (ψ) were 90 and 3°, respectively. An accurate hole Ø 5 mm with tight tolerance was machined in sidewall of die to insert head of vibrated horn. The ultrasonic vibration was transmitted to specimen in the plastic deformation zone by sonotrode (or horn). In order to reach ideal wave transmission, it is recommended to make horn and booster by same material, so the horn was made from heat-treated aluminum 7075-T6 with good mechanical strength and high sound velocity (low density). To amplify low magnitude of vibration amplitude on the transducer, the conical type of horn with stepped head was considered. The overall length of horn was designed based on working at same resonant frequency transducer equal to ~20 kHz. Then, the modal analysis was carried out by finite element code ABAQUS/frequency to detail design of horn and find node points to fix vibrated horn. Figure 2 shows longitudinal mode shape of the designed horn at resonance frequency 20,031 Hz. As shown in this figure, the longitudinal displacement contour confirms an amplification ~2.5 times in vibration amplitude in horn tip. The fabricated horn was fastened from indicated node point (zero vibration) on support structure with two flexible O-rings on both sides. After fixing of horn ring in node point, the actual resonance frequency of fabricated horn in free vibration condition was measured equal to 20,055 Hz that showed a good agreement with the designed one.

The actual vibration amplitude on the horn head needs to be indicated for adjusting input voltage to reach desirable amplitude. Therefore, an accurate Gap-Sensor (Applied

Table 1 Chemical composition and mechanical properties of commercially pure aluminum (As annealed)

Element	AL	Si	Fe	Cu	Zn	Mg	Mn	Other
Used (% wt)	Base	0.072	0.462	0.014	0.018	0.011	0.008	0.011
Mechanical properties	Yield strength (MPa)		Density (Kg/m^3)		Elastic modulus (GPa)		Poison ration	
Value	12		2700		E = 69, G = 26		0.33	

Electronics Corp.) was used to measure vibration displacement on the horn head. The simple block diagram of measuring system is shown in Fig. 3a schematically. In this way, the actual sinusoidal displacement of horn head is recorded in the oscilloscope. Figure 3b illustrates the measured vibration amplitudes in different input voltages. The fitted curve confirms the linear behavior of amplitude-voltage relationship.

2.3 Test procedure

Figure 4a illustrates block diagram of experimental setup with indicated input data and outputs. The three main tooling components of experimental setup for UE process including ultrasonic equipments, designed horn, and the developed die were assembled to apply ultrasonic vibration in vertical direction (V-UE) against extrusion direction as shown in Fig. 4b. In other setup, the assembled die lies on the bed horizontally to impose vibration in lateral direction (L-UE). The assembled die was mounted on the bed of pressing machine. The aluminum samples were polished and lubricated by MoS2 grease for reducing tribological condition occurred by miniaturization. A 30-ton (Instron 8502) press machine was used to run experiments. The punch velocity was 5 mm/min. The high-frequency voltage generated by 3 kW ultrasonic generator (Model: KRF-1500) fed to a piezoelectric transducer. In the second step, the ultrasonic vibration was imposed by horn through the designed cylindrical hole to the sample directly. The different vibration amplitudes 4, 8, 12, 15, and 20 μm were set by various input voltages. Also, the conventional ECAE without vibration test was executed while the generator was turned off. All processed samples were cut in two directions parallel (X–Y plane) and perpendicular (Y–Z plane) to extrusion axis as shown in Fig. 4a. These sectioned parts were cold mounted, electro-polished, and etched for microstructural investigations by optical micrograph (OM) and scanning electron microscopy (SEM) methods. Also, the microhardness tests were performed by Wolpert testing machine using Vickers indenter with a load of 100 g for a period of 10 s. Also, the processed bars with dimensions $5 \times 4 \times 20$ mm^3 were prepared after conventional and ultrasonic-assisted ECAE for plane strain compression (PSC) tests. Finally, the test data records including forming force measurement, compression strength curve, microhardness values, and OM and SEM images will be analyzed and discussed in next section.

3 Results and discussion

3.1 Forming load

The measured forming force versus stroke during ECAE processes without (means CE process) and with ultrasonic excitation in two different vibration (means L-UE and V-UE) have been plotted in Fig. 5a. The UV at resonance condition $f \sim 20$,

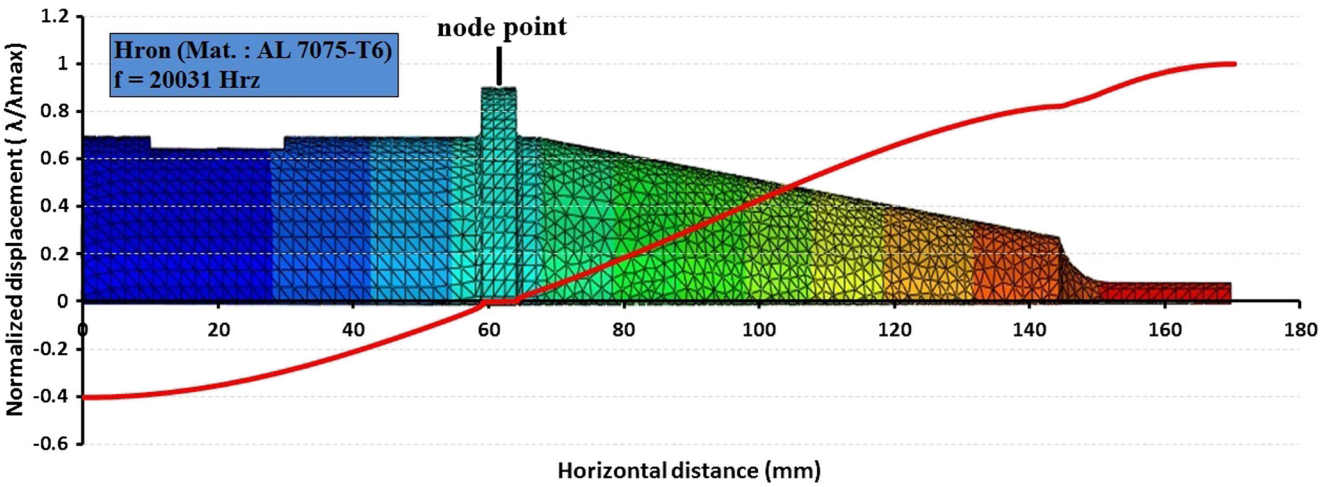

Fig. 2 Modal analysis of the designed horn

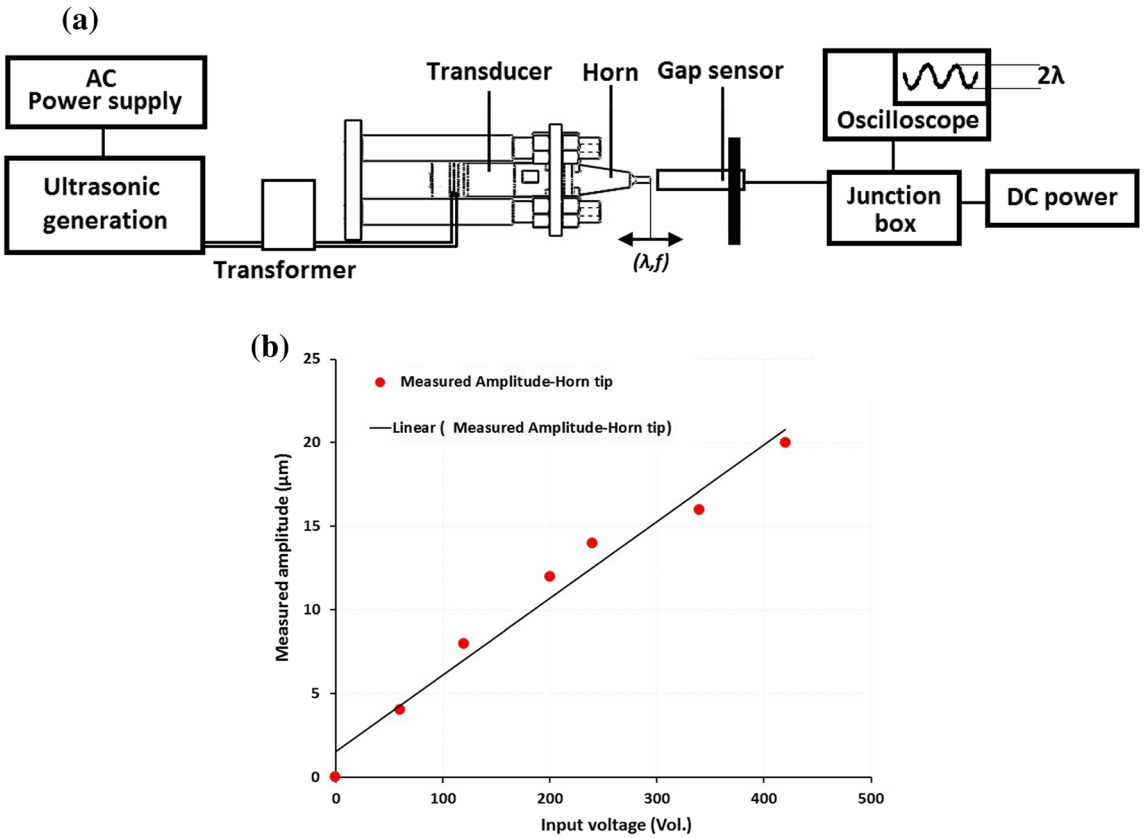

Fig. 3 **a** The schematic view of measuring system examined by gap sensor. **b** The measured amplitude-voltage curve (linear fitting)

400 Hz with amplitude $\lambda = 20$ μm was applied during UE processes. As shown in this figure, the forming force during ECAE process increases during deformation until it reach to a stable level called mean forming force. A typical rise in forming force curves after fixing load is probably related to slight flash formation in the billet walls during ECAE processes. The average forming force ~7.1 kN for CE decreases to ~6.2 kN (14 % reduction) and ~5.5 kN (30 % reduction) when ultrasonic vibration was applied in lateral (L-UE) and vertical (V-UE) directions, respectively. This decrement can be explained by both key effects of UV combined by plastic deformation including acoustic softening of material and friction force reduction between billet and horn/die. A comparative analysis between required deformation power in ECAE without and with assisting ultrasonic energy can be drawn by considering deformation energy (J) expression given by [10]:

$$J = \int_V \overline{\sigma}\dot{\overline{\varepsilon}}_p dV + \int_{Sv} \overline{\tau}|v|ds - \int_{St} T_i v_i ds \tag{3}$$

where $\overline{\sigma}$ and $\overline{\tau}$ are the yield stresses in tension and shear respectively, $\dot{\overline{\varepsilon}}_p$ is the equivalent plastic strain rate, $|v|$ is the velocity discontinuities, and T_i are the tractions given on S_t. Based on decrease in flow strength ($\overline{\sigma}$) as well as frictional shear stress reduction ($\overline{\tau}$) due to using UV, one expects that the total deformation power and resultant forming force decrease during UE compared to the CE process. In addition, the results show a superior load reduction when ultrasonic vibration applied vertically (V-UE) due to superimposing acoustic pressure against extrusion direction. This imposed acoustic pressure can be estimated by $P = \lambda.\omega.\rho.c$ [22], where λ, ω, ρ, and c are vibration amplitude, angular frequency, density of metal, and sound velocity on metal, respectively. The estimated acoustic pressure for used aluminum material with $\rho = 2700\ \mathrm{kg/m^3}$, $c = \sqrt{E/\rho} = 5055\ m/s$, $\lambda = 1.5 \times 10^{-5} m$ and $\omega = 2\pi f = 125663\ 1/s$ will be around 25 MPa. In addition, in V-UE method, friction force will be aligned with extrusion direction when the vibration was applied in reverse extrusion direction. Figure 5b illustrates the mean values of forming force after first and second passes of conventional ECAE and ultrasonic assisted ones as V-UE and L-UE with the amplitude $\lambda = 15$ μm. The fluctuation bound of forming force around mean value due to applying vibration has been indicated too. As it can be seen from recorded mean values, the percentage of forming load reduction was ~30 % after first pass of V-UE method much significant than 9 % reduction reported by authors [16] in previous attempt. The forming load reduction was achieved about 14 % after second pass of V-UE. The decrease in forming load reduction in the higher passes can be explained by increasing of dislocation density in

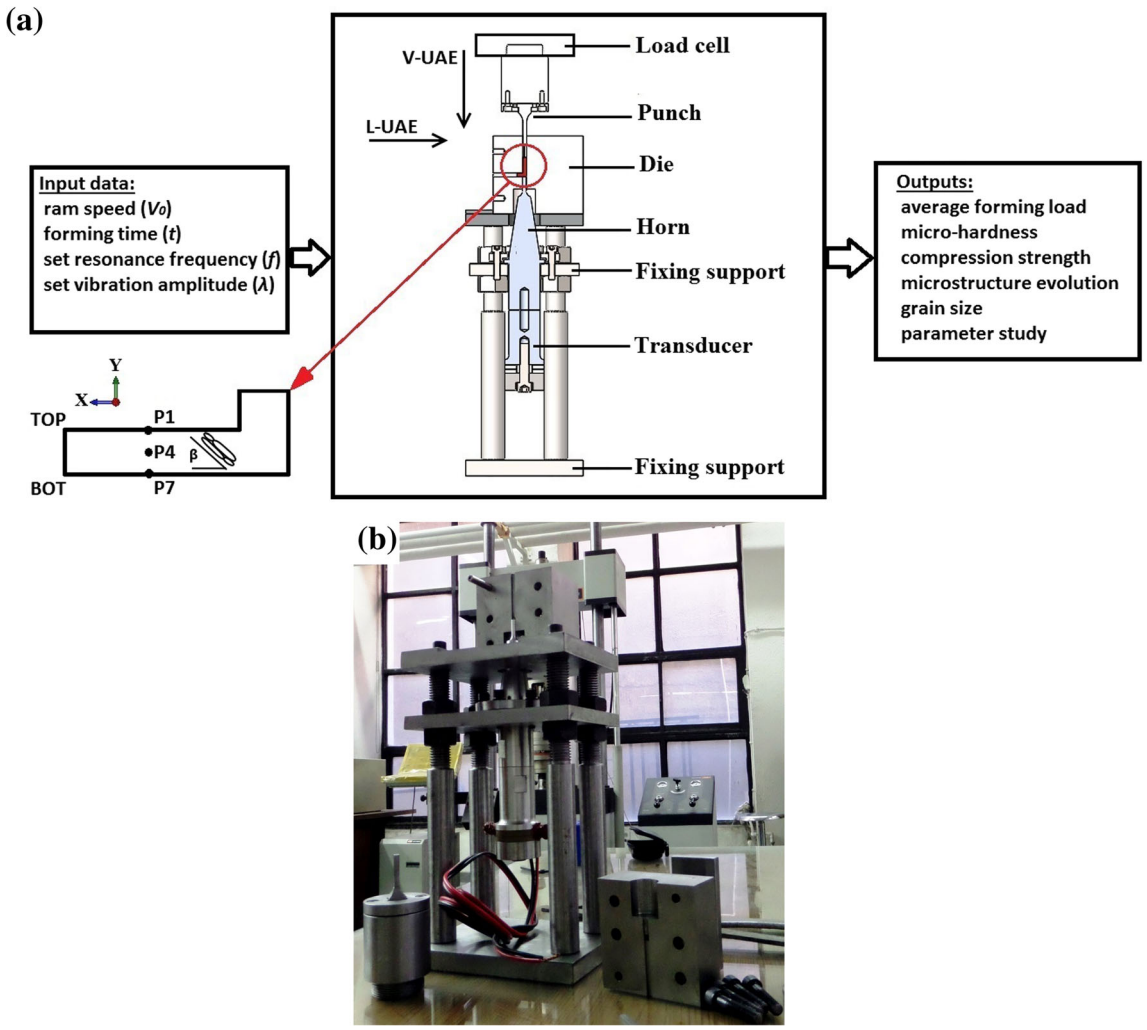

Fig. 4 **a** The block diagram of ultrasonic-assisted ECAE test. **b** The V-UE test components

higher passes of ECAE. This means that the acoustic softening phenomenon during ultrasonic excitation of metal has been less active in the higher passes of ECAE because of the large amount of tangled dislocations and residual hardening of

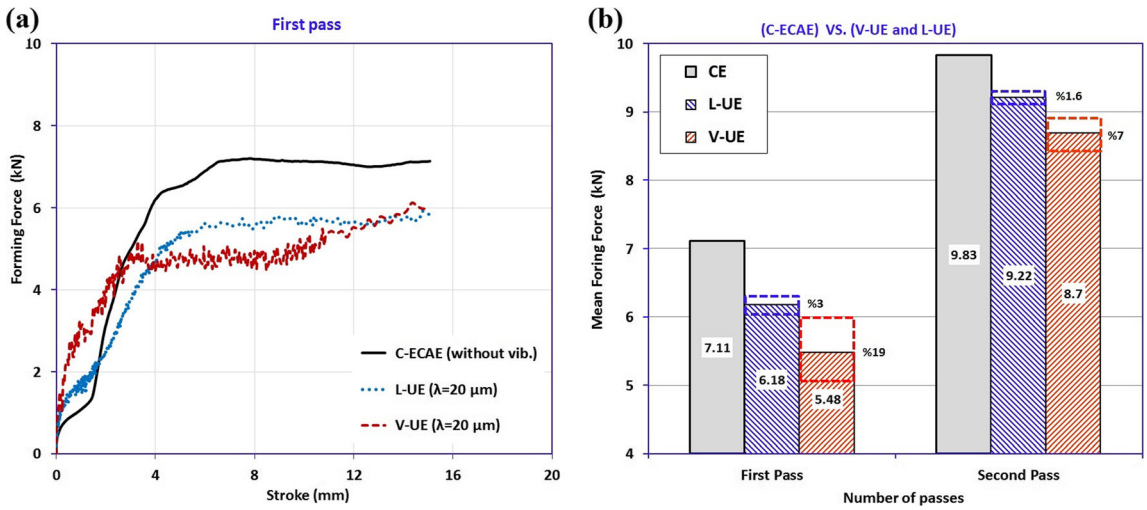

Fig. 5 **a** The forming load during CE (without vibration), V-UE, and L-UE processes ($\lambda = 20$ μm). **b** Comparison of the average forming load for first and second passes ($\lambda = 15$ μm)

material probably. Also, the scattering of forming force in terms of mean load percentage is 19 and 3 % for V-UE and L-UE that reduces to 7 and 1.6 % for the second pass. The load fluctuation is negligible in L-UE process. In addition, it can confirm the significant effect of superimposed vibrational force on the forming load reduction in V-UE than L-UE caused due to vibration direction. The fluctuation of load during V-UE method is proportional to applied vibration amplitude, and it decreases in higher passes due to vibration damping occurs in the higher value of forming load.

Figure 6 shows the average required forming loads for pressing of aluminum sample during one pass of the CE without vibration and UE processes with ultrasonic vibration. As shown in this figure, the lower required force is needed to press sample by using ultrasonic. Also, the effect of vertical vibration (V-UE) is more significant than lateral ultrasonic one (L-UE) when the same vibration amplitude was imposed. Even in small magnitude of amplitude means $\lambda = 4$ μm, the force reduction ~15 % occurred when the vertical vibration was applied while the force reduction was negligible in lateral vibration one at same amplitude. In fact, unlike lateral vibration of billet in the PDZ without back pressure, the material experiences punch pressure against vertical ultrasonic vibration in the V-UE method effectively. This may be the reason why the acoustic softening and the more forming force reduction were detected when ultrasonic vibration was plied vertically. In addition, the increment of vibration amplitude value leads to more forming load reduction. A notable forming force reduction, 37 and 24 %, happened when the maximum amplitude $\lambda = 20$ μm was irradiated as vertically and laterally, respectively. In fact, the acoustic softening effect, as a dominant volume effect due to the high-frequency vibration, increased with increasing vibration amplitude as reported in literature

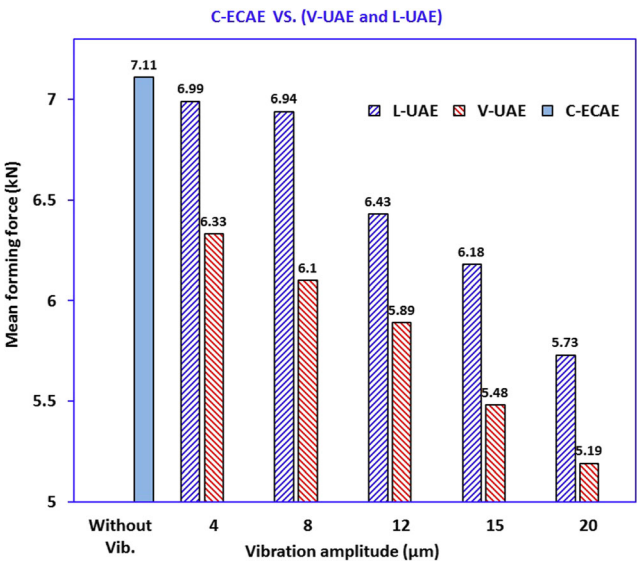

Fig. 6 The mean required forming load during conventional and various amplitudes of ultrasonic ECAE

works. The mean forming load decrease due to the acoustic softening during the vibration was found to be linearly proportional to the vibration amplitude, which was observed in flow stress reduction of ultrasonic assisted compression tests as well [6, 19].

3.2 Microhardness and compression tests

The distribution of the mean microhardness values in the processed samples through billet thickness is illustrated in Fig. 7a. These values have been recorded from point 1 (top surface) up to point 7 (bottom surface) from steady-state region of the product samples, as indicated in Fig. 4b. The ultrasonic-assisted ECAE tests in both vibration directions were performed with constant amplitude $\lambda = 15$ μm. As expected, the hardness value increased remarkably after conventional ECAE process from initial mean value of ~24 Hv for initial annealed sample to ~41 Hv. As shown in this figure, the hardness curves have been raised when the ultrasonic vibration was used. The mean value of hardness increased to ~48 and ~51 Hv after using ultrasonic vibration in lateral and vertical direction, respectively, so the UE-processed samples showed about 24 % improvement in hardness than CE process. The increase of microhardness in the samples processed using ultrasonic propagation seems to be attributed to more grain refinement as a result of dislocation density rise and subgrain boundaries formation. The nearly same hardness promotion has been reported in [23] by four passes ECAP of pure aluminum 1050. In addition, the use of ultrasonic vibration as vertical direction (V-UE) shows higher hardness values with more uniform distribution than L-UE after one pass. It means that although the values of hardness is increased, more homogeneous hardness distribution is obtained by applying ultrasonic vibration in the opposite direction of extrusion direction. The standard error about 7, 6, and 3 % from measured values for each point in CE, L-UE, and V-UE can also prove the better homogeneity in V-UE method. Also, it is interesting to note that the value of micro-hardness in the bottom surface of both samples processed by two various methods of UE were similarly ~52 Hv. Formation of the ultrasonic-irradiated bottom surface with high strength after L-UE method can be found while the V-UEed sample shows a nearly uniform strength distribution. The comparison of mean micro-hardness values of samples after first and second passes of CE, L-UE, and V-UE has been illustrates in Fig. 7b. The results show nearly the same increasing trend in microhardness after second pass of CE and both UT methods. Of course, it is interesting to note that the hardness value of samples with ultrasonic irradiation after first pass was still greater than CE sample after second pass, so it can be concluded that the use of ultrasonic vibration can decrease the number of ECAE passes to reach high strength products effectively.

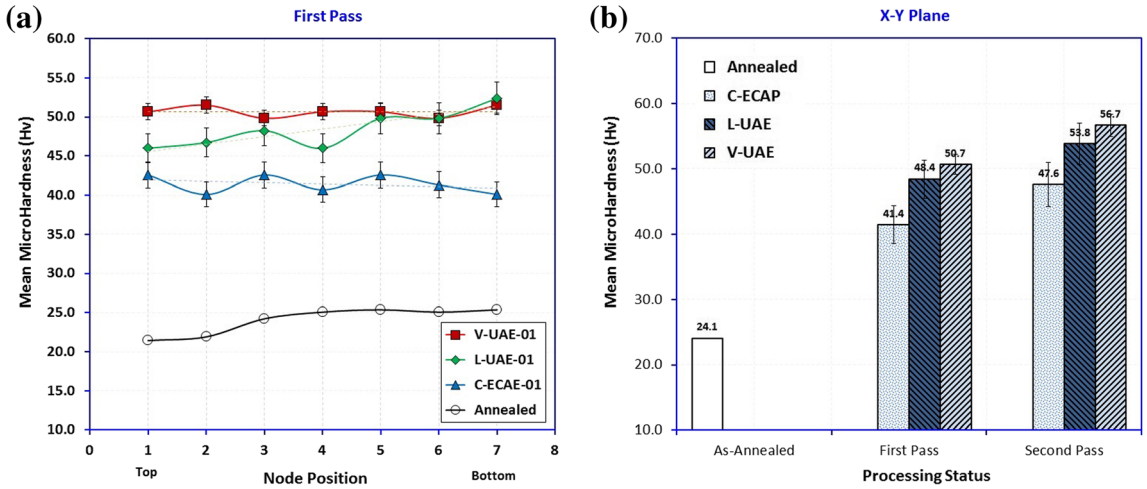

Fig. 7 **a** The microhardness variation on X–Y plane of samples after first pass of CE, L-UE, and V-UE processes. **b** Comparison of the mean microhardness values after first and second passes

Because of small dimension of products, the compressive strength of processed samples after one pass of CE, L-UE, and V-UE was examined by plane strain compression (PSC) test. An often technique used to enforce a plane strain compression was pressing of bar in a channel, as shown schematically in Fig. 8a [24]. In this test, the walls suppress lateral straining ($\varepsilon_{zz} \simeq 0$), and the indentor and lateral walls restrict shear in X-plane ($\varepsilon_{yz} \simeq 0$), but the other shear components ε_{xz} and ε_{xy} are free to occur, so the significant stress in this test will be compression stress σ_{yy}. The dimensions of sample test was $5 \times 4 \times 20$ mm^3, and PSC test was performed at strain rate $\dot{\varepsilon} \approx 2 \times 10^{-2}\ (1/s)$. The sample bar surfaces and walls are well lubricated. The pressing speed was 5 mm/min for compression ratio %50. The compression force was recorded for each test samples. Figure 8a shows the compression behavior of the as-annealed and ECAEed without and with ultrasonic excitation specimens after one pass. As expected, due to severe plastic deformation, the conventional ECAE process leads to an increase in the flow stress level and compression strength of initial sample. In addition, a slight improvement in compressive strength of products processed by ECAE with ultrasonic vibration (L-UE and V-UE) can be seen. For example, as seen in Fig. 8b, the flow stress at strain value 2 % was measured 22, 24, and 25 MPa for CE, L-UE, and V-UE specimens than 9 MPa in the initial billet. The slight rise in the compression strength of samples processed by ECAE with ultrasonic irradiation can be explained by further grain refinement and also residual acoustic hardening effect which occurs when vibration is turned off [6, 19]. Of course, the better conclusion can be figured

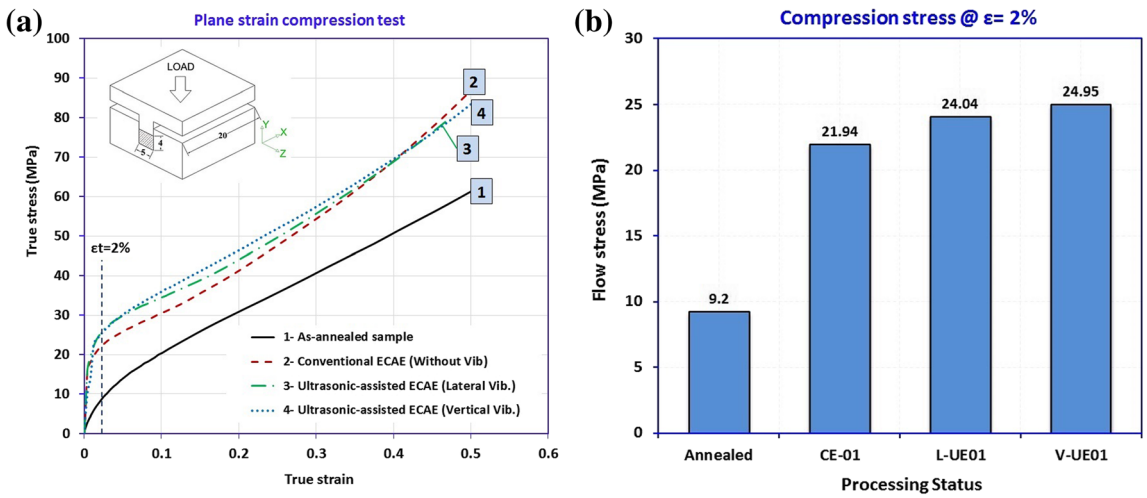

Fig. 8 **a** True stress-strain curves of processes samples by CE, L-UE, and V-UE processes. **b** Flow stress values of samples at strain $\varepsilon = 0.02$

out by using tensile tests with large dimensions of product samples.

3.3 Microstructure characteristics

The initial annealed specimen with three processed samples after first pass of ECAE without and with ultrasonic irradiation was sectioned on the X–Y plane for optical microscopy (OM) study. All samples were investigated in the middle of thickness (point "4"), as indicated in Fig. 4b. Figure 9a illustrates OM image of initial sample after annealing treatment with nearly equiaxed grains with size ~160 μm. Figure 9b–d shows the microstructural change after first pass of conventional ECAE and ultrasonic-assisted ECAE processes with both vibration directions. Figure 9b corresponds to sample after conventional ECAE without ultrasonic vibration. There are elongated grains with non-uniform distribution due to shearing deformation mode. The mean grain size after one pass of CE was ~25 μm which is obtained by averaging between width and length of elongated grains. As expected, several passes of CE process are necessary to reach a homogenous equiaxed fine-grained structure. Figure 9c, d illustrates microstructure of processed aluminum using ultrasonic vibration ($f = 20$ kHz and $\lambda = 15$ μm). As shown in these images, greater grain refinement can be observed in the processed samples with both L-UE and V-UE methods. In the sample processed with lateral ultrasonic excitation (L-UE method), still some elongated coarse grains (ECG) with localized regions with equiaxed fined grains (EFG) can be seen, as indicated in Fig. 9b, which represent nearly inhomogeneity in the structure. However, the microstructure of sample processed with vertical ultrasound irradiation (V-UE method) illustrates more grain refinement with better uniformity (Fig. 9c). This phenomenon can be explained by increasing dislocation density in plastic deformation zone and/or the shearing and subdivision of elongated grains severely due to applying high-intensity ultrasonic vibration. However, this superimposed vibrational pressure acts more effective in V-UE than L-UE due to existing back extrusion pressure opposite to vertical vibration direction. In addition, the OM images of samples after ECAE show formation of grains along a special angle called grain elongation angle (β), which occur along many shear planes in succession. As shown in Fig. 4a, the angle β is measured rather than x-axis for dominant elongated grains. The approximate measured angle β was 32, 19, and 44° for CE, L-UE, and V-UE processed samples, respectively. In fact, the applied vibrational pressure during UE process causes change in grains rotation in the PDZ. Hence, the severe compressed grains in PDZ during V-UE method demonstrate greater inclination than those formed by lateral ultrasonic propagation (L-UE) as reported similarly in [25] for structures with different aspect ratio factors. Based on

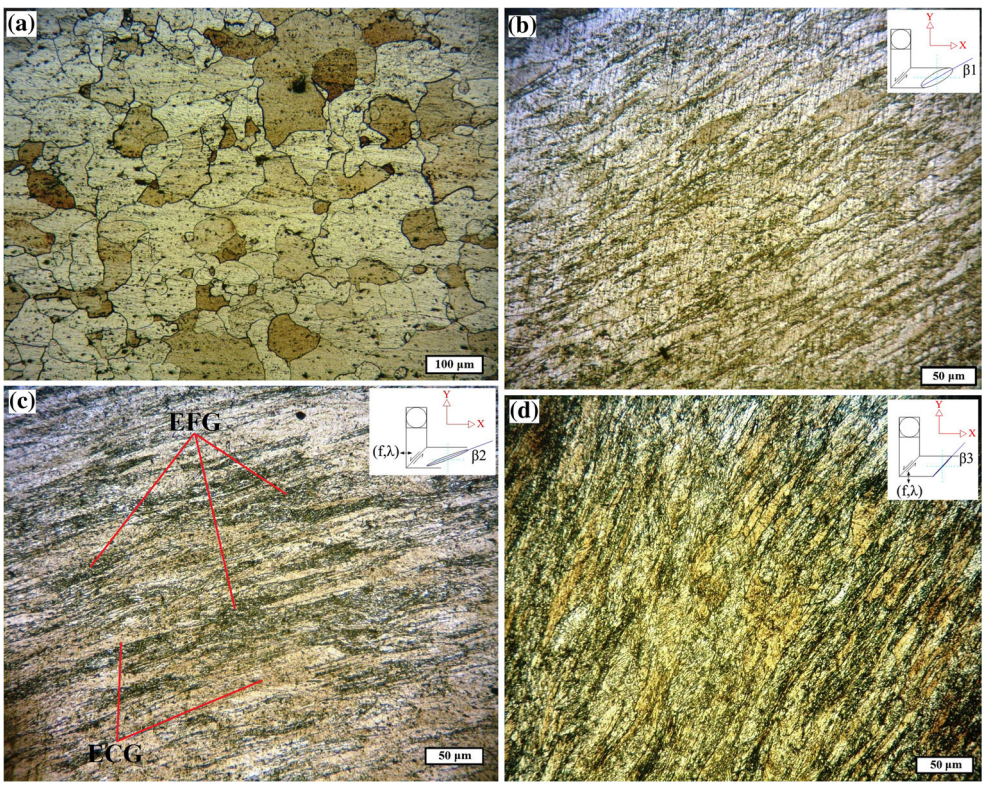

Fig. 9 Microstructure of the pure aluminum samples for **a** as-annealed initial, processed samples after one pass of **b** CE, **c** L-UE, and **d** V-UE processes

that, it is reasonable to expect that the nearly equiaxed grains with more rotation in PDZ were formed during L-UE versus elongated inclined grains in the V-UE.

Table 2 compares results of present work with those obtained by previous researchers on ECAE process of pure aluminum. In the present study, the elongated grains with size ~25 μm after one pass of CE method were refined into small equiaxed grains with size ~5 μm after second pass of CE via route C that is above the result reported by [26]. The localized smaller grains with equiaxed shape can be seen in the sample processed by UE method. The scanning electron microscope (SEM) machine was utilized to evaluate grain size in the localized area of samples. Figure 10 shows the SEM micrograph of sample after one pass of UE process (similarly with $f = 20$ kHz and $\lambda = 15$ μm).

It is demonstrated that using ultrasonic vibration contributes to grain refinement most efficiently leading to formation of almost equiaxed shape ultra-fined grains (UFG) with average grain size ~2 μm. The equiaxed grains have been obtained with average grain size 4 μm after two passes of CE via route C [26] and grains with size about 2.3 μm after four passes of CE process via route C [27]. It shows capability of the present method in grain refinement of pure aluminum clearly. As reported by Langdon [28], it may be difficult to achieve equiaxed grain boundaries structure with routes A and C compare to route Bc. Via route Bc, the equiaxed grains with size 2.1 μm were observed after two passes of CE [23] nearly similar to result was observed in the present study after one pass of V-UE process. Although some elongated grains can be seen in Fig. 10, that means inhomogeneity in the microstructure, several passes of V-UE method can improve homogeneity of structure. Comparing the results as summarized in Tables 2 reported by previous researchers, two and four passes of CE and the one pass of UE sample can draw a conclusion to improve efficiency of ECAE for decreasing of the required process passes by using high-intensity ultrasonic vibration. Results exhibit also higher mechanical properties promoted by the developed microstructure in samples processed by UE method.

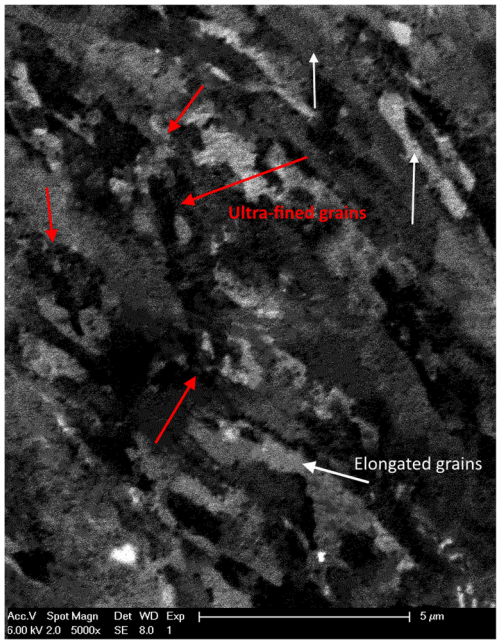

Fig. 10 SEM micrograph from localized area of sample processed by ultrasonic-assisted ECAE

4 Conclusion

In this research, an experimental investigation on the effect of combining high-intensity ultrasonic vibration with equal channel angular extrusion (UE) in two directions was conducted to improve some limitations of conventional ECAE (CE) method. The obtained results from CE and UE methods can be drawn as follows:

- The required forming force of ECAE process decreases by using ultrasonic vibration as 30 and 14 % in the V-UE and L-UE methods, respectively, in comparison with CE method. Of course, the force reduction was 15 % for second pass of V-UE due to increase in dislocation density in higher passes.
- The forming force reduction rises with increasing vibration amplitude for example required forming force decreases from 6.33 to 5.2 kN by applying amplitude 4

Table 2 Comparison of hardness and grain size in the present work with those obtained by other researchers on CE process of pure aluminum

Material & ref.	Process	Die angle	Route	No. of passes	Hardness (Hv)	Grain size (μm)	
						Initial	After
Pure AL 99.5 % [26]	CE	$\Phi = 90°$, $\psi = 10°$	C	2	–	150	4
Pure AL 1050 [27]	CE	$\Phi = 90°$, $\psi = 0°$	C	4	54	300	2.3
Pure AL 1050 [23]	CE	$\Phi = 90°$, $\psi = 0°$	Bc	2	50	600	2.1
Pure AL1050, Present work	CE	$\Phi = 90°$, $\psi = 3°$	C	2	~48	160	~5
Pure AL1050, Present work	V-UE	$\Phi = 90°$, $\psi = 3°$	–	1	~51	160	~2

and 20 μm for V-UE method, respectively. The forming force reduction is more effective in the V-UE method than L-UE.

- The hardness of UEed samples increases to 48 Hv (for L-UE) and 51 Hv (for V-UE) than initial value 24 Hv versus the mean value 41 Hv for CE processed sample. These UE processed samples show greater hardness values even than CEed sample after two passes with hardness value 47.6 Hv.
- The results of plane strain compression test prove a slight improvement in compression strength of samples processed by UE than CE ones. The flow stress increases by ~2.5 times in the UEed samples than initial billet. Of course, the tensile test can reveal strength enhancement better, which will be possible in the samples with large dimensions.
- The nearly equiaxed grains with average grain size ~2 μm were obtained after one pass of UE method by imposing UV with amplitude $\lambda = 15$ μm. The grain refinement is more effective in the presented method than two and four passes of CE method via route C. The obtained result is almost similar to observed grains with size 2.1 μm by two passes of CE via route Bc [23].
- These findings show the effective role of applying ultrasonic vibration in ECAE process to improve some of its limitations including forming force reduction, mechanical properties enhancement, and decrease of ECAE passes to reach UFG structure.

Acknowledgments SB acknowledges for financial support in part from Iran Nanotechnology Initiative Council (INIC). All technical supports and facilities provided by University of Teheran and Purdue University to conduct this research are gratefully acknowledged. SB also acknowledges Dr. Wilson Xu and Dr. Xiaoming Wang (Purdue University-West Lafayette, USA) for the fruitful ideas about study on microstructural characteristics.

References

1. Hall EO (1951) The deformation and ageing of mild steel: III discussion of results. Proc Phys Soc 64:747–753
2. Segal VM (1995) Materials processing by simple shear. Mater Sci Eng A 197:157–164. doi:10.1016/0921-5093(95)09705-8
3. Valiev RZ, Langdon TG (2006) Principles of equal-channel angular pressing as a processing tool for grain refinement. Prog Mater Sci 51:881–981. doi:10.1016/j.pmatsci.2006.02.003
4. Siddiq A, El Sayed T (2012) Ultrasonic-assisted manufacturing processes: variational model and numerical simulations. Ultrasonics 52:521–529. doi:10.1016/j.ultras.2011.11.004
5. Bagherzadeh S, Abrinia K, Han Q (2016) Ultrasonic assisted equal channel angular extrusion (UAE) as a novel hybrid method for continuous production of ultra-fine grained metals. Mater Lett 169:90–94. doi:10.1016/j.matlet.2016.01.095
6. Bagherzadeh S, Abrinia K (2015) Effect of ultrasonic vibration on compression behavior and microstructural characteristics of commercially pure aluminum. J Mater Eng Perform. doi:10.1007/s11665-015-1730-8
7. Langenecker B (1966) Effects of ultrasound on deformation characteristics of metals. IEEE Trans Sonics Ultrason SU-13:1–8
8. Yin F, Hu S, Hua L, Wang X, Suslov S, Han Q (2014) Surface nanocrystallization and numerical modeling of low carbon steel by means of ultrasonic shot peening. Metall Mater Trans A Phys Metall Mater Sci 46:1253–1261. doi:10.1007/s11661-014-2689-z
9. Jimma T, Kasuga Y, Iwaki N, Miyazawa O, Mori E, Ito K, Hatano H (1998) An application of ultrasonic vibration to the deep drawing process. J Mater Process Technol 80–81:406–412. doi:10.1016/S0924-0136(98)00195-2
10. Bunget C, Ngaile G (2011) Influence of ultrasonic vibration on micro-extrusion. Ultrasonics 51:606–616. doi:10.1016/j.ultras.2011.01.001
11. Han Q, Xu C, Jian X (2007) Method of producing nanostructured metals using high-intensity ultrasonic vibration. 1–5
12. Wen T, Wei L, Chen X, Pei C (2011) Effects of ultrasonic vibration on plastic deformation of AZ31 during the tensile process. Int J Miner Metall Mater 18:70–76. doi:10.1007/s12613-011-0402-4
13. Siu KW, Ngan AHW, Jones IP (2011) New insight on acoustoplasticity–ultrasonic irradiation enhances subgrain formation during deformation. Int J Plast 27:788–800. doi:10.1016/j.ijplas.2010.09.007
14. Liu Y, Suslov S, Han Q, Xu C, Hua L (2012) Microstructure of the pure copper produced by upsetting with ultrasonic vibration. Mater Lett 67:52–55. doi:10.1016/j.matlet.2011.08.086
15. Han Q (2015) Ultrasonic processing of materials. Metall Mater Trans B 46:1603–1614. doi:10.2172/859314
16. Djavanroodi F, Ahmadian H, Koohkan K, Naseri R (2013) Ultrasonic assisted-ECAP. Ultrasonics 53:1089–1096. doi:10.1016/j.ultras.2013.02.003
17. Liu Y, Suslov S, Han Q, Hua L, Xu C (2013) Comparison between ultrasonic vibration-assisted upsetting and conventional upsetting. Metall Mater Trans A 44:3232–3244. doi:10.1007/s11661-013-1651-9
18. Siddiq A, El Sayed T (2011) Acoustic softening in metals during ultrasonic assisted deformation via CP-FEM. Mater Lett 65:356–359. doi:10.1016/j.matlet.2010.10.031
19. Yao Z, Kim G, Wang Z, Faidley L, Zou Q, Mei D, Chen Z (2012) Acoustic softening and residual hardening in aluminum: modeling and experiments. Int J Plast 1–13. doi:10.1016/j.ijplas.2012.06.003
20. Hess DP, Soom A, Kim CH (1992) Normal vibrations and friction at a Hertzian contact under random excitation: theory and experiments. J Sound Vib 153:491–508. doi:10.1016/0022-460X(92)90378-B
21. Kumar V, Hutchings I (2004) Reduction of the sliding friction of metals by the application of longitudinal or transverse ultrasonic vibration. Tribol Int 37:833–840. doi:10.1016/j.triboint.2004.05.003
22. Blitz J (1971) Ultrasonics: methods and applications. Newnes-Butterworth, p 160
23. El-Danaf EA (2008) Mechanical properties and microstructure evolution of 1050 aluminum severely deformed by ECAP to 16 passes. Mater Sci Eng A 487:189–200. doi:10.1016/j.msea.2007.10.013
24. Wonsiewicz BC, Chin GY, Hart RR (1971) Lateral constraints in plane strain compression of single crystals. Metall Mater Trans B 2:2093–2096. doi:10.1007/BF02917536
25. García-Infanta JM, Swaminathan S, Carreño F, Ruano OA, McNelley TR (2008) Grain shape and microstructural evolution during equal channel angular pressing. Scr Mater 58:17–20. doi:10.1016/j.scriptamat.2007.09.007
26. Kim KJ, Yang DY, Yoon JW (2010) Microstructural evolution and its effect on mechanical properties of commercially pure aluminum deformed by ECAE (equal channel angular extrusion) via routes A

and C. Mater Sci Eng A 527:7927–7930. doi:10.1016/j.msea.2010.08.084

27. El-Danaf EA, Soliman MS, Almajid AA, El-Rayes MM (2007) Enhancement of mechanical properties and grain size refinement of commercial purity aluminum 1050 processed by ECAP. Mater Sci Eng A 458:226–234. doi:10.1016/j.msea.2006.12.077
28. Langdon TG (2007) The principles of grain refinement in equal-channel angular pressing. Mater Sci Eng A 462:3–11